Article

Dynamic Interplay between Diffusion and Reaction: Nitrogen Recombination on Rh{211} in Car Exhaust Catalysis

Oliver R. Inderwildi, Stephen J. Jenkins, and David A. King

J. Am. Chem. Soc., **2008**, 130 (7), 2213-2220 • DOI: 10.1021/ja0754913

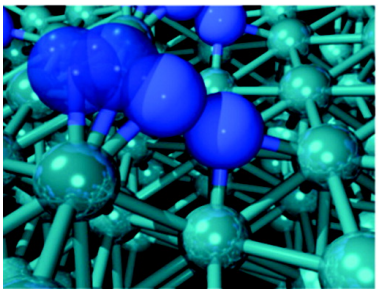

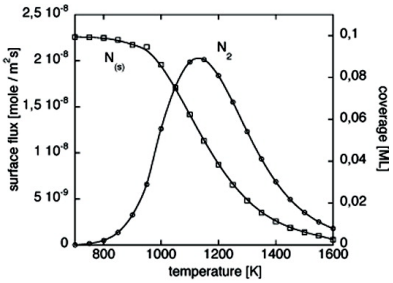

More About This Article

Additional resources and features associated with this article are available within the HTML version:

- Supporting Information
- Links to the 2 articles that cite this article, as of the time of this article download
- Access to high resolution figures
- Links to articles and content related to this article
- Copyright permission to reproduce figures and/or text from this article

View the Full Text HTML

J|A|C|S
ARTICLES
Published on Web 01/25/2008

Dynamic Interplay between Diffusion and Reaction: Nitrogen Recombination on Rh{211} in Car Exhaust Catalysis

Oliver R. Inderwildi,* Stephen J. Jenkins, and David A. King

University of Cambridge, Department of Chemistry, Lensfield Road, Cambridge CB2 1EW, United Kingdom

Received July 23, 2007; E-mail: ori20@cam.ac.uk

Abstract: The adsorption and diffusion of atomic nitrogen on Rh{211} as well as formation and desorption of molecular nitrogen from this surface have been investigated by means of density functional theory (DFT) calculations. The elementary step reaction mechanism derived from this comprehensive DFT study forms the foundation of a detailed microkinetic model including diffusion, recombination, and desorption of nitrogen species. It will be shown that nitrogen formation on a stepped rhodium surface is a dynamic interplay of atomic nitrogen diffusion and reaction. Moreover, evidence will be presented that not one but several on-step recombination reactions are responsible for dinitrogen formation and desorption.

1. Introduction

The purification of automobile exhaust gases is a widespread research topic.[1−6] In the case of conventional engines, which are operated under stoichiometric conditions, NO_x ($x = 1, 2$) is removed efficiently using a so-called 3-way catalyst;[2,7−9] the component responsible for the removal of NO_x is rhodium.[2] On rhodium surfaces, NO_2 deoxygenates readily to NO, which in turn is able to decompose on surface defects such as steps to form atomic nitrogen as well as oxygen.[10] The oxygen formed is removed by oxidation reactions,[11] and nitrogen is, presumably, able to recombine to form molecular N_2. In more fuel-efficient engines, such as for instance the Diesel engine, this system is not applicable, since these engines are operated with an excess of oxygen (lean-burn conditions) and rhodium would be poisoned by adsorbed atomic oxygen under these conditions. Moreover, the amount of reductants present in the exhaust stream is lower, preventing removal of the oxygen from the surface. If, however, short reductant-rich phases are periodically induced in the exhaust gas stream, efficient conversion of NO_x to N_2 is possible.[12,13]

To understand the mechanism of this conversion on a metal surface, three processes have to be taken into account: (1) decomposition of NO; (2) recombination of atomic nitrogen to N_2; and (3) oxygen removal from the surface (provision of vacant sites). The catalytic cycle of NO_x reduction on a precious metal surface according to Burch et al.[14] is given in Figure 1.

Although surface decomposition of NO has to date been studied extensively by means of DFT[4,10,15−20] and Monte Carlo simulations based on DFT results,[21−24] the recombination of atomic nitrogen has received little attention. Ample et al. studied the recombination of atomic nitrogen on Rh{111} and from this work it can be concluded that this surface facet is absolutely inactive with respect to dinitrogen formation at the relevant temperatures (roughly below 600 K).[25] Hermse et al. were able to reproduce results for temperature programmed desorption (TPD) experiments of nitrogen from Rh{111} using kinetic Monte Carlo simulations.[26] In their study, barriers were estimated based on the Brønsted-Evans-Polanyi (BEP) relation-

(1) Garin, F. *Catal. Today* **2004**, *89*(3), 255−268.
(2) Chatterjee, D.; Deutschmann, O.; Warnatz, J. *Faraday Discuss.* **2001**, *119*, 371−384.
(3) Broqvist, P.; Panas, I.; Gronbeck, H. *J. Phys. Chem. B* **2005**, *109*(19), 9613−9621.
(4) Liu, Z. P.; Jenkins, S. J.; King, D. A. *J. Am. Chem. Soc*. **2003**, *125*(48), 14660−14661.
(5) Wogerbauer, C.; Maciejewski, M.; Baiker, A.; Gobel, U. *Top. Catal*. **2001**, *16*(1−4), 181−186.
(6) Strobel, R.; Krumeich, F.; Pratsinis, S. E.; Baiker, A. *J. Catal*. **2006**, *243*(2), 229−238.
(7) Taylor, K. C. *Catal. Rev.* **1993**, *35*(4), 457−481.
(8) Engler, B. H. *Chem. Ing. Tech*. **1991**, *63*(4), 298−&.
(9) Miyamoto, A.; Inoue, B.; Murakami, Y. *Ind. Eng. Chem. Prod. Res. Dev.* **1979**, *18*(2), 104−109.
(10) Inderwildi, O. R.; Lebiedz, D.; Deutschmann, O.; Warnatz, J. *ChemPhysChem* **2005**, *6*(12), 2513−2521.
(11) Inderwildi, O. R.; Jenkins, S. J.; King, D. A. *J. Am. Chem. Soc*. **2007**, *129*(6), 1751−1759.
(12) Nakatsuji, T.; Komppa, V. *Appl. Catal. B* **2001**, *30*(1−2), 209−223.
(13) Nakatsuji, T.; Komppa, V. *Catal. Today* **2002**, *75*(1−4), 407−412.
(14) Burch, R.; Millington, P.; Walker, A. *Appl. Catal. B* **1994**, *4*(1), 65−94.
(15) Loffreda, D.; Simon, D.; Sautet, P. *J. Catal.* **2003**, *213*(2), 211−225.
(16) Loffreda, D.; Simon, D.; Sautet, P. *J. Chem. Phys*. **1998**, *108*(15), 6447−6457.
(17) Loffreda, D.; Delbecq, F.; Simon, D.; Sautet, P. *J. Chem. Phys*. **2001**, *115*(17), 8101−8111.
(18) Liu, Z. P.; Jenkins, S. J.; King, D. A. *J. Am. Chem. Soc*. **2004**, *126*(34), 10746−10756.
(19) Inderwildi, O. R.; Lebiedz, D.; Warnatz, J. *Phys. Chem. Chem. Phys*. **2005**, *7*(13), 2552−2553.
(20) Gonzalez, S.; Sousa, C.; Illas, F. *J. Catal*. **2006**, *239*(2), 431−440.
(21) van Bavel, A. P.; Hermse, C. G. M.; Hopstaken, M. J. P.; Jansen, A. P. J.; Lukkien, J. J.; Hilbers, P. A. J.; Niemantsverdriet, J. W. *Phys. Chem. Chem. Phys.* **2004**, *6*(8), 1830−1836.
(22) Hopstaken, M. J. P.; Niemantsverdriet, J. W. *J. Chem. Phys*. **2000**, *113*(13), 5457−5465.
(23) Hopstaken, M. J. P.; Niemantsverdriet, J. W. *J. Vac. Sci. Tech. A* **2000**, *18*(4), 1503−1508.
(24) Hopstaken, M. J. P.; Niemantsverdriet, J. W. *J. Phys. Chem. B* **2000**, *104*(14), 3058−3066.
(25) Ample, F.; Ricart, J. M.; Clotet, A.; Curulla, D.; Niemantsverdriet, J. W. *Chem. Phys. Lett*. **2004**, *385*(1−2), 52−54.
(26) Hermse, C. G. M.; van Bavel, A. P.; Nieuwenhuys, B. E.; Lukkien, J. J.; van Santen, R. A.; Jansen, A. P. J. *Langmuir* **2005**, *21*(18), 8302−8311.

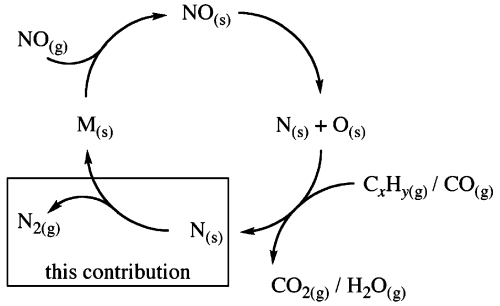

Figure 1. Catalytic cycle of the decomposition of NO and its conversion into molecular nitrogen on a metal surface, the so-called Burch mechanism.[14]

ship[19,27,28] and one recombination reaction at step sites was considered. In the present study, by contrast, all the diffusion processes and different recombination reactions as well as desorption reactions are accurately determined by DFT calculations. This comprehensive DFT study forms the basis for a detailed elementary-step microkinetic model of N_2 formation at a vicinal rhodium surface. The interplay of diffusion and reaction on the stepped surface is investigated, and it will be shown that for an elementary-step study the assumption of one on-step recombination reaction is simply not good enough. This study is the first step in a systematic and comprehensive study of NO_x reduction under constant lean and alternating lean-rich conditions. In further steps we will gauge the influence of oxygen on the recombination reaction of nitrogen, the reaction of oxygen with nitrogen surface species and also study the removal of oxygen from the steps by oxidation reaction. Ricart et al. have shown previously that oxygen might have an influence on the nitrogen formation.[29]

2. Computational Method

In this work, the adsorption, diffusion, recombination, and desorption of dinitrogen on a {211} facet of rhodium were studied by means of DFT calculations using the CASTEP computer code.[30] The generalized gradient approximation (GGA) as proposed by Perdew et al. was applied,[31] combined with Vanderbilt ultrasoft pseudopotentials.[32] The planewave basis set was truncated at a kinetic energy of 340 eV. The Brillouin zone was sampled by a *k*-point mesh with a *k*-point spacing of below 0.05 $Å^{-1}$, as generated by the Monkhorst−Pack scheme[33] (the mesh used for a (2 × 1) elementary cell is hence a 3 × 4 × 1 mesh). The surface was modeled using an eight-layer rhodium slab, with the lower five layers fixed at their bulk positions and the uppermost three layers mobile. Previous studies have shown that this thickness is sufficient for the simulation of surface processes.[34] Periodic boundary conditions were used to model an extended surface and a 10 Å vacuum region was placed between the periodically repeated slabs to ensure that the adsorbate and the subsequent slab do not interact. Adsorption energies are calculated according to

$$E_{ad} = E_{surface+xN} - \left(E_{surface} + \frac{x}{2}E_{N_2}\right) \quad (1)$$

in which $E_{surface+xN}$ stands for the total energy of nitrogen adsorbed on Rh{211} and E_{N_2} stands for the total energy of isolated molecular nitrogen in the same elementary cell used for the surface calculations; adsorption energies are hence referenced to molecular nitrogen in the gas phase.

The transition states of the surface reactions/transformations were located on the potential energy surface (PES) by performing linear synchronous and quadratic synchronous transit calculations with conjugate gradient refinements.[35] All transition states were converged using this procedure until a root-mean-squared gradient of less than 0.15 $eVÅ^{-1}$ was reached. Conjugate gradient refinement was used to ensure that the transition state found is a first-order transition state, by verifying that the transition state is a minimum in all direction conjugate to the reaction coordinate.

The diffusion and desorption of nitrogen on and from Rh{211} was simulated using the DETCHEM software package by Deutschmann et al.,[36] based on an elementary-step reaction-diffusion mechanism derived from plane-wave DFT calculations. DETCHEM uses an Arrhenius-type equation for the determination of the surface diffusion coefficient of each migration step. The diffusion coefficient k_d is calculated according to

$$k_d = \upsilon_0 \exp\left(-\frac{E_m}{RT}\right) \quad (3)$$

where ν_0 is the attempt frequency, commonly associated with the lateral vibrational mode of the adatom, and E_m is the activation barrier for the surface migration, that is, a site jump. The lateral vibrational mode is commonly assumed to be 10^{13} Hz, a typical surface phonon frequency,[37,38] which is also in agreement with transition state theory. In case of association, the rate k_a is calculated according to

$$k_a = A \exp\left(-\frac{E_a}{RT}\right) \quad (4)$$

The attempt frequency derived for transition state theory is used as pre-exponential factor *A* in the Arrhenius expression, as in the case of diffusion (for a comprehensive diffusion study using this setup, see ref 39). In the presented case, diffusion and association are related because a collision that leads to association is a diffusion process as well. The crucial difference in the case of a diatomic surface recombination is that a recombination process ends up with an atom moving into an already occupied site (and hence leads to formation of N_2), while a diffusion process ends up with an adatom in a previously unoccupied site (and hence does not lead to a chemical reaction).

Desorption of a species *i* is described analogously to eq 3; the pre-exponential factor in this case is also the attempt frequency υ_0, and the activation barrier for desorption was calculated by means of DFT.

$$k_{des} = \upsilon_0 \exp\left(-\frac{E_a}{RT}\right) \quad (5)$$

Using these rate coefficients, the production rate $\dot{s}_i$ of a surface or gas-phase species *i* can then be calculated according to

$$\frac{ds}{dt} = \sum_{k=1}^{K_s} \upsilon_{ik} k_{fk} \prod_{i=1}^{N_G+N_S} c_i^{\upsilon'_{ik}} \quad f = \text{des, d, a} \quad (6)$$

(27) Michaelides, A.; Liu, Z. P.; Zhang, C. J.; Alavi, A.; King, D. A.; Hu, P. *J. Am. Chem. Soc.* **2003**, *125*(13), 3704−3705.
(28) Bligaard, T.; Norskov, J. K.; Dahl, S.; Matthiesen, J.; Christensen, C. H.; Sehested, J. *J. Catal.* **2004**, *224*(1), 206−217.
(29) Ricart, J. M.; Ample, F.; Clotet, A.; Curulla, D.; Niemantsverdriet, J. W.; Paul, J. F.; Perez-Ramirez, J. *J. Catal.* **2005**, *232*(1), 179−185.
(30) Segall, M. D.; Lindan, P. J. D.; Probert, M. J.; Pickard, C. J.; Hasnip, P. J.; Clark, S. J.; Payne, M. C. *J. Phys − Cond. Matt.* **2002**, *14*(11), 2717−2744.
(31) Perdew, J. P.; Chevary, J. A.; Vosko, S. H.; Jackson, K. A.; Pederson, M. R.; Singh, D. J.; Fiolhais, C. *Phys. Rev. B* **1992**, *46*(11), 6671−6687.
(32) Vanderbilt, D. *Phys. Rev. B* **1990**, *41*(11), 7892−7895.
(33) Monkhorst, H. J.; Pack, J. D. *Phys. Rev. B* **1976**, *13*(12), 5188−5192.
(34) Rasmussen, M. D.; Molina, L. M.; Hammer, B. *J. Chem. Phys.* **2004**, *120*(2), 988−997.
(35) Govind, N.; Petersen, M.; Fitzgerald, G.; King-Smith, D.; Andzelm, J. *Comp. Mat. Sci.* **2003**, *28*(2), 250−258.
(36) Deutschmann, O. http://www.detchem.com, 2001.
(37) Ratsch, C.; Scheffler, M. *Phys. Rev. B* **1998**, *58*(19), 13163−13166.
(38) Swartzentruber, B. S. *Phys. Rev. Lett.* **1996**, *76*(3), 459−462.
(39) Inderwildi, O. R.; Kraft, M. *ChemPhysChem* **2007**, *8*(3), 444−451.

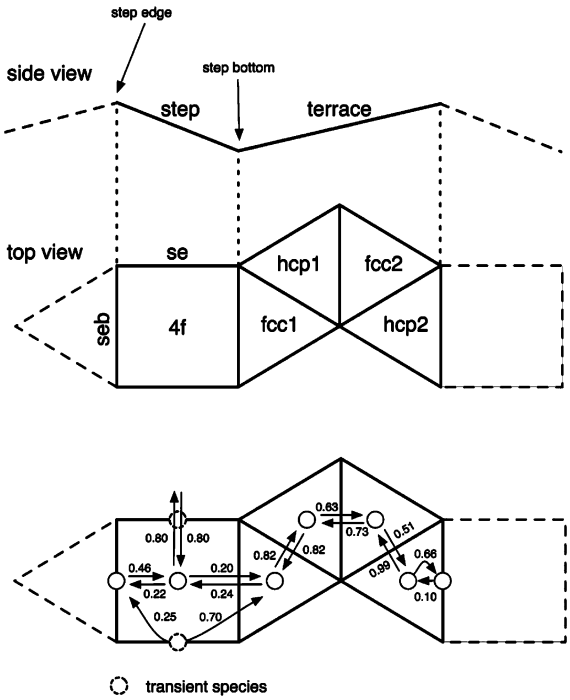

Figure 2. (Top) Schematic of the elementary cell of an fcc {211} surface, possible adsorption sites for N labeled (4f: fourfold-hollow, seb: step-edge bridged, sb: step-bridged); the subsequent elementary cell are indicated by gray, dotted lines. (Bottom) Possible single-site jumps for atomic nitrogen; migration barriers are given in eV next to the arrow describing the migration.

in which K_S is the number of surface reactions and N_G and N_S are the number of gas-phase and surface species respectively. The concentration of a species i (or coverage in the case of a surface species) is denoted as c_i and the stoechiometric factor of species i in reaction k is denoted υ_{ik}. The possible sites for diffusion are explained in the text; for the details of the implementation of DETCHEM, see ref 40.

3. Results and Discussion

3.1. Adsorbed Atomic Nitrogen on (1 × 2)-Rh{211}. Prior to calculating surface transformations and reactions, the adsorption of atomic nitrogen on (1 × 2)-Rh{211}, corresponding to an atom coverage of 0.167 ML, was studied. (There are two common nomenclatures for the coverage of a surface: in one, a full monolayer corresponds to one atom or molecule in a (1 × 1) elementary cell. In the other, a full monolayer coverage is reached when there is one adsorbate atom bound to every surface atom. In the former nomenclature, the term coverage is ambiguous, because it has to be clarified whether an atomic or molecular coverage is meant. The latter nomenclature, however, does not suffer from this disadvantage, and because we are here dealing with formation of molecules from atoms, the latter nomenclature is chosen for convenience.) There are several possibilities for adsorption in three-, four-, and two-fold positions, whereas atop adsorption sites can be neglected as can bridged adsorption sites on the terrace. The upper scheme in Figure 2 gives an overview over the different possible adsorption sites; the adsorption energies are given in Table 1. As can be seen from this table, by far the most stable adsorption site is the three-fold site adjacent to the descending step edge (hcp2).

Table 1. Adsorption Energies of Atomic Nitrogen on (1 × 2)-Rh{211} with Respect to Molecular Nitrogen

site	E_{ad} [eV]
sb	0.53
seb	−0.04
fcc1	−0.24
hcp1	−0.25
fcc2	−0.14
hcp2	−0.61
4f	−0.27

It is, however, known that NO decomposes preferentially when adsorbed on the terrace adjacent to the ascending step edge,[10,15] which means that atomic nitrogen is formed on the other side of the terrace, i.e., on the fcc1 and potentially also on the hcp1 position.

Also, the fourfold hollow position on the step is slightly more stable than the fcc1 position. This immediately suggests that nitrogen might diffuse readily to the hcp2 position via the {100} step at the temperatures necessary for NO decomposition. Moreover, to recombine, some of the nitrogen on the surface must be located at the step or on the step edge, making the diffusion on this stepped surface even more interesting.

3.2. Diffusion of N on Rh{211}. To investigate the rearrangement of atomic nitrogen formed by NO decomposition, the possible surface migration processes were examined. The transition states of the single-site jumps between neighboring stable adsorption geometries were determined. They are summarized in Figure 2, lower panel. In brief, diffusion via the terrace should be negligible at lower temperatures, whereas diffusion from fcc1 toward the most stable site (hcp2) via the step should be possible. Site jumps in which the transition state is located in atop position (as for instance a site jump from hcp2 to fcc1) can be neglected in the temperature range investigated, because N in the atop position is energetically highly unfavorable.

To verify the proposed kinetics, diffusion was investigated using the barriers determined by DFT. The starting point of the kinetic simulation is a surface covered with 0.1 ML atomic nitrogen. All the nitrogen is initially placed in the fcc1 position, because it is known that NO decomposes preferentially from this position and hence atomic nitrogen will be formed there.[41] The evolution of the surface overlayer with increasing temperature was simulated neglecting association. This approximation is justifiable for an initial survey as at such a low coverage and temperature the probability of collision and recombination is relatively negligible. The temperature range investigated spans from temperatures relevant for surface science investigations (i.e., below 300 K) to temperatures relevant for real-world applications (i.e., up to 600 K). As can be seen from Figure 3, diffusion from fcc1 to the fourfold hollow site starts at 120 K, the "light-off" of this process is at 200 K. The concentration of N adsorbed in fourfold hollow sites (4f) on the step peaks at 230 K. Above this temperature, an equilibrium between the fcc1 and 4f site is established, as can be seen from Figure 3. This equilibrium shifts toward the fcc1 site with increasing temperature until diffusion from the 4f site to the hcp2 site sets in at 320 K. Diffusion from 4f to hcp2 proceeds via the step-edged bridged position; the population of this site is, however,

(40) Schwiedernoch, R.; Tischer, S.; Correa, C.; Deutschmann, O. *Chem. Eng. Sci.* **2003**, *58*(3−6), 633−642.

(41) Inderwildi, O. R.; Jenkins, S. J.; King, D. A. unpublished, 2007.

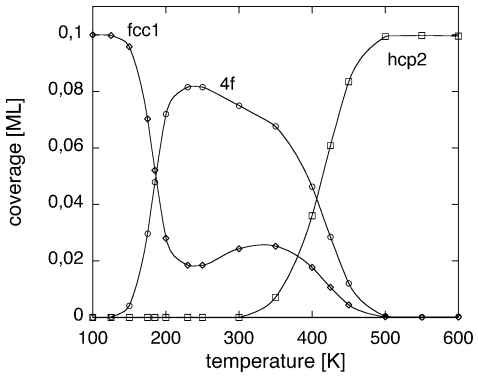

Figure 3. Evolution of 0.1 ML nitrogen with the temperature starting form the fcc1 position, the surface population after 50 s is given; the nomenclature is given in Figure 2, top panel.

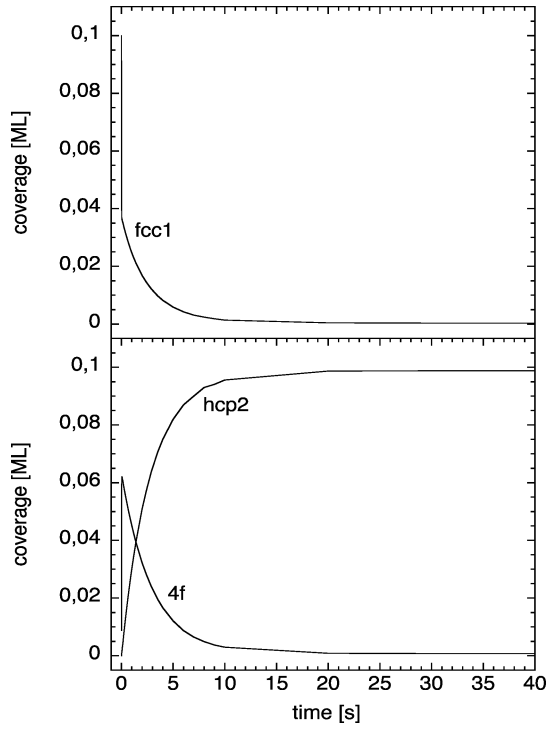

Figure 4. Transient evolution of 0.1 ML nitrogen at 600 K starting from a coverage of 0.1 in the fcc1position, the preferred position for N formation by NO decomposition.

negligible as all the atoms that can cross the 0.2 eV barrier to this position can also overcome the 0.1 eV barrier to the most stable hcp2 site. At approximately 550 K, all nitrogen atoms have reached the hcp2 position.

To investigate what happens to a nitrogen atom formed in an on-step NO decomposition under exhaust-gas catalysis relevant conditions (600 K), the transient evolution of the surface overlayer was simulated. As can be seen from Figure 4, nitrogen leaves the fcc1 position immediately; after only 1 s, more than 60% of the nitrogen atoms reside in the fourfold hollow position on the step. This site only acts as an intermediate for the diffusion to the hcp2 position. All atoms also diffuse via the step-edge bridge position, and the barrier for diffusion from this site to the much more stable hcp2 site is so low (0.1 eV) that the population of this site is negligible. After 20 s, the system reaches its equilibrium with 99% of all nitrogen atoms adsorbed in the hcp2 position and only 1% adsorbed in fourfold hollow position. These results suggest that a recombination mechanism suggested previously for Ir,[18] in which nitrogen from fcc1 and seb positions combine to adsorbed N_2, is not a likely pathway in case of rhodium. To evaluate where molecular nitrogen is formed, different recombination reactions on step and terrace were considered in this work.

Moreover, the fast diffusion of nitrogen from the fcc1 to the hcp2 position is interesting, because this process removes the nitrogen from the base of the step, the active sites for NO decomposition. After nitrogen has diffused to hcp2 on the step edge, NO can adsorb and subsequently decompose from its preferred adsorption site, the fcc1 site. Atomic nitrogen adsorbed in the hcp2 position does not hinder the NO decomposition according to our calculations.[41] This mechanism would also implicitly explain how two nitrogen atoms can be located at a step facing each other even though diffusion along the {111} direction is negligible: After a first NO decomposition, the produced oxygen is removed via an oxidation reaction, and subsequently N diffuses to the hcp2 position. After a further NO decomposition and O removal reaction, two N's would be located facing each other (fcc1, hcp2) at the step, from where they could recombine.

3.3. Adsorption of Dinitrogen on Rh{211}. To determine the strength of the bonding of dinitrogen to the Rh{211} surface, and its dependence on the nitrogen coverage, the adsorption energy of the molecule at different coverage was calculated. This was done by determining different stable adsorption geometries of N_2 on Rh{211}. Because initial calculations have shown that the position in which the N_2 is located on the step with its axis normal to the ridge (Figure 7) is by far the most stable adsorption site, it was assumed that this is the only site to consider for the coverage dependence study.

A (1 × 4) elementary cell was created and one to four dinitrogen molecules were placed on the step, corresponding to coverages of 0.08, 0.17, 0.25, and 0.33 ML. A coverage of 0.33 ML represents a Rh{211} surface with the step fully covered with dinitrogen molecules (a dinitrogen adsorbed occupies two surface sites). For 0.33, 0.25 and 0.08 ML there is only one possible adsorption structure, while in case of 0.16 there are two. At this coverage the dinitrogen molecules can either be separated by one vacant site (Figure 5b) or can reside next to each other leaving a gap of two vacant adsorption sites Figure 5c).

The energy of desorption of one N_2 molecule at 1 ML is 0.43 eV; if a molecule desorbs from the 0.75 ML covered Rh{211} (Figure 5d) it can either be the middle one, leading to the more stable alternating structure (Figure 5b), or one of the outer dinitrogens, leading to the less stable structure (Figure 5c). Consequently, the first desorption is energetically more favorable with a desorption energy of 0.05 eV, while the latter is less favorable with a desorption energy of 0.44 eV. Desorption of a further molecule from the structure in Figure 5b requires 1.1 eV, and from structure in Figure 5c requires 0.7 eV. Both desorptions lead to a surface covered with 0.25 ML dinitrogen; desorption from this structure requires 0.99 eV. Based on these DFT results, it can be concluded that, in the case of this (1 × 4) elementary cell, dinitrogen will mainly desorb in the following order e → d → b → a (Figure 5). In the (unlikely) case that the structure in Figure 5c is formed desorption will follow the order e → d → c → a. The former pathway is named path A in Figure 6, the latter is named path B. From this plot

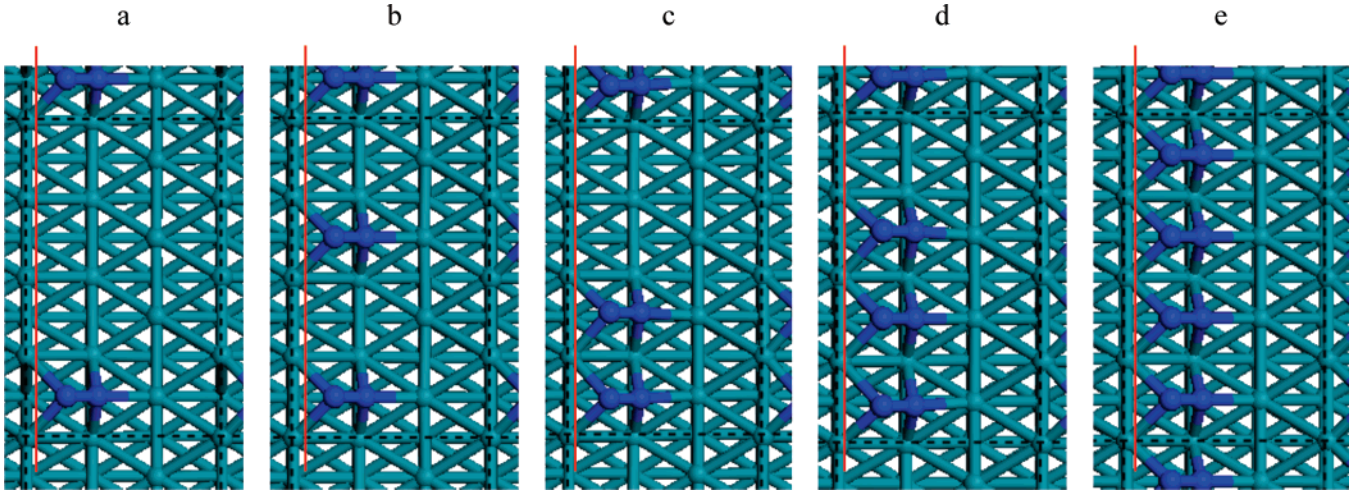

Figure 5. Different possible adsorption structures of N_2 on Rh{211} at 0.08 (a), 0.16 (b, c), 0.25 (d) and 0.33 ML (e); the step-edge is indicated with a red line; the (100) step is immediately to the right of this line.

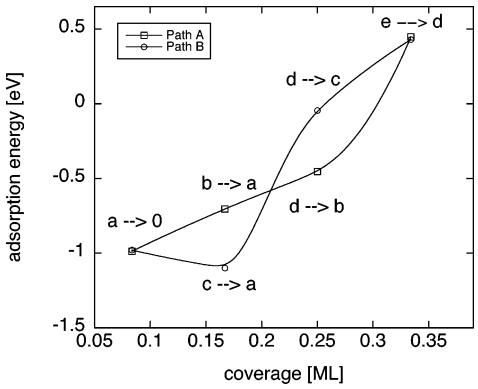

Figure 6. Energy change of dinitrogen on (4 × 1)-Rh{211} as a function of the coverage, the corresponding structures are given in Figure 5; adsorption of two dinitrogen can lead to two different adsorption structures b and c; adsorption of a further dinitrogen leads to structure d, but has different adsorption energies via path A or B.

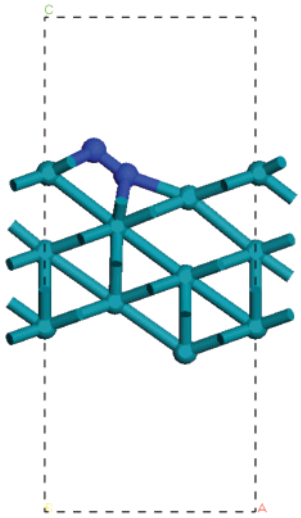

Figure 7. Molecular nitrogen adsorbed on-step on Rh{211}.

it can also be seen that dinitrogen will not be present in high concentrations at step sites, owing to the exothermicity of desorption. The exothermic desorption from the fully covered rhodium step seems to be due to stress induced by repulsion of the coadsorbed N_2 molecules: the distance between adjacent N_2 molecules is 2.69 Å in the case of the fully covered surface step, but when one N_2 is removed however the two outer dinitrogens relax outward thereby increasing the spacing to 2.86 Å, an increase of 6.3%. The outer two dinitrogens are therefore slightly displaced from their symmetric adsorption position, which is compensated by the lower lateral repulsion. The outer two dinitrogens are 5.72 Å apart in this adsorption structures (Figure 5d). Upon desorption of the middle dinitrogen, the most likely desorption, the outer two dinitrogens relax back into the symmetric adsorption position and the spacing reduces from 5.72 to 5.38 Å, because bonding competition and lateral repulsion vanish (Figure 5b).

3.4. Association Reaction. To verify where gaseous N_2 is formed from atomic nitrogen on this stepped surface, the different likely possibilities on Rh{211} were investigated. Usually, decomposition reactions are investigated in DFT studies starting from the most stable adsorption site. In this case, however, this would mean that N_2 is produced on the {111} terrace of Rh{211}. This would be reasonable if Rh{111} is a good catalyst for nitrogen association, which seems unlikely based on previous DFT[25] and experimental studies.[42] We therefore studied the association of nitrogen from various local minima on the Rh{211} surface.

On the terrace adjacent to the bottom of the step, the transition states look quite similar to those on Rh{111}[25] (Figure 8, parts 1 and 2); also the activation barriers (1.59 and 1.60 eV) are in agreement with previous studies on Rh{111} by Ample *et alia*.[25] The only difference to Rh{111} is that here the N_2 formed directly rearranges to an on-step adsorption site (Figure 7). This also makes the reaction more exothermic than on the terrace sites adjacent to the step-edge, where the N_2 formed is adsorbed on the flat terrace. Association on the terrace adjacent to the step-edge has a similarly high activation barrier (1.69 eV) and is in addition not as exothermic as the other on-step association reactions (Figure 8, part 3). Activation barriers and energies of reaction are given in Table 2.

On the step, the barriers toward recombination of N are considerably lower. By far the lowest energy pathway is the recombination of N located on the seb position, with a N located on the fcc1 position. The activation barrier for this process is 0.31 eV, the transition state is depicted in Figure 8, part 4.

(42) Zaera, F.; Gopinath, C. S. *J. Chem. Phys.* **2002**, *116*(3), 1128−1136.

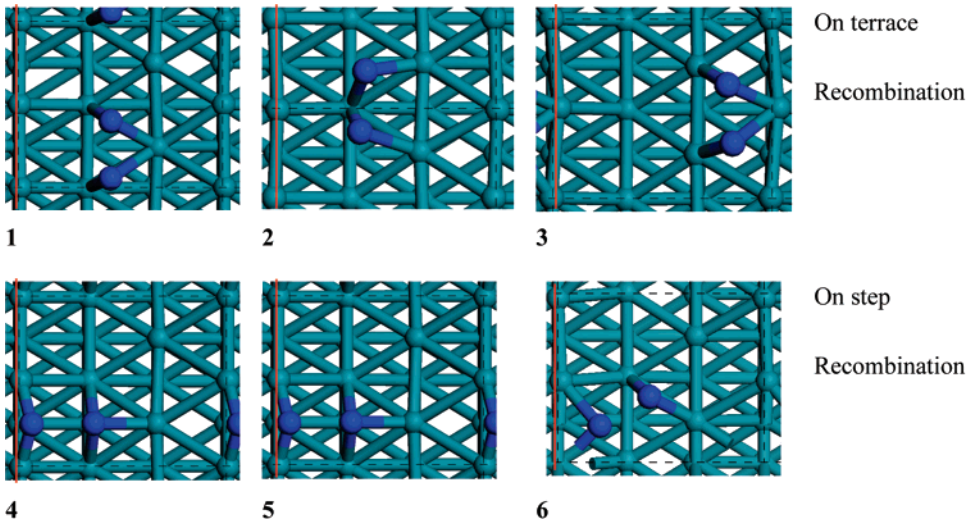

Figure 8. Transition states of the different N association reactions on Rh{211}; numbering in Table 2; the step edge is indicated with a red line; the (100) step is immediately to the right of this line.

Table 2. Reaction Energies and Activation Barriers for the Association of Atomic to Molecular Nitrogen on Rh{211}[a]

	reaction	E_A [eV]	ΔE [eV]
1.	$N_{(fcc1)} + N_{(fcc1)} \rightarrow N_{2(s)} + 2\,Rh_{(fcc1)}$	1.60	−0.74
2.	$N_{(hcp1)} + N_{(hcp1)} \rightarrow N_{2(s)} + 2\,Rh_{(hcp1)}$	1.59	−0.57
3.	$N_{(hcp2)} + N_{(hcp2)} \rightarrow N_{2(s)} + Rh_{(hcp2)} + Rh_{(hcp2)}$	1.69	−0.18
4.	$N_{(seb)} + N_{(fcc1)} \rightarrow N_{2(s)} + Rh_{(seb)} + Rh_{(fcc1)}$	0.35	−0.87
5.	$N_{(4f)} + N_{(hcp2)} \rightarrow N_{2(s)} + Rh_{(4f)} + Rh_{(hcp2)}$	0.91	−0.3
6.	$N_{(4f)} + N_{(hcp1)} \rightarrow N_{2(s)} + Rh_{(4f)} + Rh_{(hcp1)}$	1.10	−0.83

[a] $N_{2(s)}$ refers to moleular nitrogen adsorbed on the step.

However, the microkinetic model of nitrogen diffusion, *vide supra*, has shown that coverages on these sites are rather low, excluding it as the main reaction pathway. Moreover, it is difficult to explain how this adsorption arrangement materializes. First, diffusion of N into this arrangement is unlikely, owing to the high diffusion barriers along the <110> coordinate on the terrace as well as on the step edge. Second, direct formation of N in the seb position is unlikely due to the high decomposition barrier (2.91 eV[41]). Third, direct formation of N in the fcc1 position is not possible, because the seb site (the site to which O would decompose) is blocked. Therefore, alternative pathways for the recombination of nitrogen have to be considered.

Other possibilities for on-surface recombination are a reaction of N from an hcp2 position with N from a 4f position. Our DFT calculations showed that this process is activated by 0.91 eV (transition state Figure 8, part 5), much higher than the seb-fcc1 recombination reaction. However, coverages are much higher in these sites and this configuration is formed easily, *vide supra*. Therefore, the actual desorption mechanism might involve a competition between diffusion and recombination reaction. Moreover, these results suggest that in different temperature regimes different mechanisms might play a role.

Hammer suggested that the activation barrier of diatomic reactions is related to the number of metal atoms that are shared by the two reactant atoms in the transition state, most likely via the bonding competition effect.[43] In the presented case, all reactions proceeding via a transition state in which the reactant atoms share one surface atom have activation barriers around 1.6 eV, whereas the reactions in which the reactants do not share a surface atom in the transition state have barriers of 1.1 eV or lower. This is rationalized as follows: the two reactant atoms compete for electron density offered by the substrate atom, and consequently the transition state is destabilised compared to a structure in which no surface atoms are shared. Hence, our findings further confirm Hammer's hypothesis.[43]

3.5. Kinetic Modeling of Diffusion and Association of Atomic Nitrogen. First, dinitrogen formation was calculated starting from a surface covered with 0.1 ML of atomic nitrogen located in fcc1 positions, analogous to the diffusion study carried out above. In this case, almost no formation of adsorbed dinitrogen can be observed in the lower temperature range, which is in agreement with observations on Rh{111} by Zaera et al.[42] Nitrogen diffuses rapidly to the hcp2 position, but association from this position is unlikely at lower temperature owing to the high activation barrier (1.69 eV). Formation and desorption of dinitrogen only sets in at temperatures far above the relevant temperature range. The coverage of adsorbed dinitrogen is low, indicating that the rate-determining steps are surface processes, rather than desorption. Because the coverage on the step-edge bridge site (seb) are very low and the site with the highest population (hcp2) does not have a low-energy pathway for recombination, it is not immediately clear how dinitrogen is formed. This motivated us to investigate the origin of dinitrogen, and we therefore labeled N_2 formed in the different recombination reactions to distinguish between the different pathways. As can be seen from the bottom graph in Figure 9, indeed there are two main reaction pathways: (1) formation on the step, that is, recombination from fcc1 and seb; and (2) formation on the upper step edge, that is, recombination from 4f and hcp2. At lower temperature, up to ca. 1200 K, pathway 1 is predominant, whereas above 1200 K pathway 2 is predominant.

How can N_2 be formed from a seb position when the population of this surface site is almost zero? Presumably via a pre-equilibrium reaction: nitrogen adsorbed on hcp2 and seb position are in equilibrium, and this equilibrium favors the hcp2 position. The small amount of N in the seb position is, however, able to react with N adsorbed on fcc1 at low temperature, because of the small activation barrier according to

(43) Hammer, B. *Surf. Sci.* **2000**, *459*(3), 323−348.

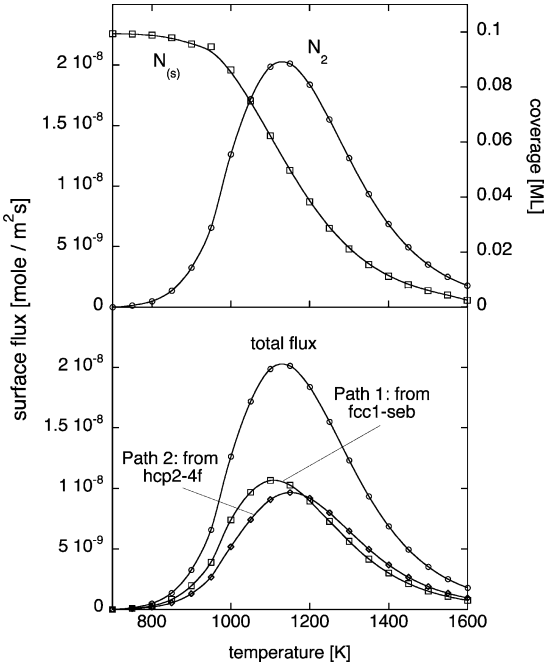

Figure 9. (Top) Simulated TPRD spectra, surface flux of dinitrogen and nitrogen coverage as a function of temperature. (Bottom) Complete surface flux and surface flux originating from different on-surface recombinations.

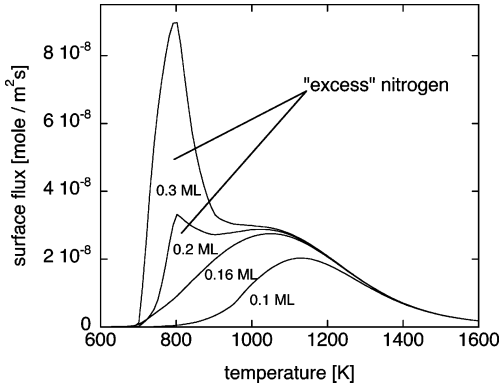

Figure 10. Simulated TPRD spectra for different initial coverages; nitrogen diffuses rapidly to the most stable hcp2 site. In cases were there is more nitrogen on the surface than the hcp2 sites can accommodate, the "excess" nitrogen remains on the step and rapidly recombines/ desorbs.

$$N_{(hcp2)} \rightleftharpoons N_{(seb)} \xrightarrow{N_{(fcc1)}} N_{2(step)} \qquad (7)$$

The amount of nitrogen formed on the terrace is absolutely negligible according to these microkinetic simulations. This supports earlier assumptions that NO is dissociated, and dinitrogen formed, at defects. This can possibly also explain the higher activity of nanoparticles in DeNOx catalysis; nanoparticles contain a higher number of defects, and therefore, the amount of active sites is higher, even though the surface area of these particles is smaller.

Theoretically, in the case of nitrogen coverages above 0.167 ML, the hcp2 sites are not able to accommodate all the adsorbed nitrogen. This would mean that the recombination via pathway 1 (from $N_{(seb)}$ and $N_{(fcc1)}$) would increase, since diffusion into and past hcp2 is blocked and the nitrogen would remain on an adsorption site on or adjacent to the step.This motivated us to simulate the TPRD spectra for different N coverages, i.e., 0.1, 0.167, 0.2 and 0.3 ML. (In case of 0.1 and 0.167 ML, the nitrogen atoms are is placed in the fcc1 position; in case of 0.2 and 0.3 ML, the nitrogen atoms are placed in the hcp1 position as well. Nitrogen is preferably formed in this position because NO decomposition is most likely here.) Indeed, our hypothesis is supported by the simulated TPRD spectra: the nitrogen atoms diffuse rapidly from the positions in which they are generated to the hcp2 position until those positions are filled. If there are more nitrogen atoms than the hcp2 position can accommodate, the "excess" nitrogen remains on the step and recombines rapidly, preferably via pathway 1. In the TPRD spectra, the desorption of these "excess" nitrogen atoms in the form of dinitrogen can be seen in the form of a sharp peak. After the excess nitrogen has left the surface, the TPRD spectra return to the bell-shaped curve. The bell-shaped parts are again due to recombination from $N_{(hcp2)}$ and $N_{(4f)}$ as well as via the pre-equilibrium.

In a realistic catalytic converter for lean-burn engines, however, the surface will have a relatively high oxygen coverage. Preliminary calculations have shown that atomic oxygen binds even more strongly to the hcp2 sites than atomic nitrogen and hence presumably blocks those, with two associated consequences. First, this might force the nitrogen formed in on-step NO dissociation onto the step and steer the reaction toward the lower energy recombination pathway (fcc1-seb). Second, preliminary results show that oxygen pre-occupation reduces the recombination barrier of nitrogen. A more comprehensive study of the interplay of atomic oxygen and nitrogen is in preparation. To understand the functioning of this system, the interplay with reductants (i.e., the removal of oxygen from the step) has to be considered on the intermediate time scale as well. In the catalytic system as proposed by Nakatsuji,[13,44] it would be conceivable that during the short rich phases oxygen is removed from defect such as steps rapidly, making them accessible for NO adsorption, decomposition, and subsequent N recombination.

4. Conclusions

We have combined DFT simulations of the adsorption, diffusion, association and desorption of nitrogen on Rh{211} with microkinetic simulations. These microkinetic simulations show that the nitrogen formation reaction is a dynamic interplay between diffusion and recombination. Furthermore, two different reaction pathways have to be considered: in pathway 1, dinitrogen is formed from a configuration which is *not* a global but only a local minimum, owing to a diffusion pre-equilibrium. In pathway 2, dinitrogen is formed via a direct reaction of coadsorbed nitrogen atoms on the step edge. Again, the reactive configuration is not a global minimum, and diffusion into this position is involved in the actual formation process. Gaseous nitrogen formation at steps is therefore a dynamic interplay between diffusion and recombination.

Moreover, this study supports previous assumptions that the selective conversion of NO to N_2 happens predominantly at surface defects (including steps), whereas plane surfaces (the

(44) Nakatsuji, T.; Ruotoistenmaki, J.; Komppa, V.; Tanaka, Y.; Uekusa, T. *Appl. Catal. B* **2002**, *38*(2), 101−116.

terrace in the presented case) are inactive. One can, however, not neglect the influence of oxygen and reductants on this reaction, which will be the topic of further studies that will broaden the present study.

Acknowledgment. We acknowledge the EPSRC and the DFG for postdoctoral fellowships (O.R.I.) and The Royal Society for a University Research Fellowship (S.J.J.). Calculations were performed on Darwin, and therefore, we are grateful to Cambridge University High Performance Computing Service.

JA0754913

(45) Mei, D. H.; Ge, Q. F.; Neurock, M.; Kieken, L.; Lerou, J. *Mol. Phys.* **2004**, *102*(4), 361−369.
(46) Hoyle, R. B.; Anghel, A. T.; Proctor, M. R. E.; King, D. A. *Phys. Rev. Lett.* **2007**, *98*(22).
(47) West, R. H.; Celnik, M. S.; Inderwildi, O. R.; Kraft, M.; Beran, G. J. O.; Green, W. H. *Ind. Eng. Chem. Res.* **2007**, *46*(19), 6147−6156.